DOI: 10.1002/chem.200800502

Azacalix[6]arene Hexamethyl Ether: Synthesis, Structure, and Selective Uptake of Carbon Dioxide in the Solid State

Hirohito Tsue,* Koichi Ishibashi, Satoshi Tokita, Hiroki Takahashi, Kazuhiro Matsui, and Rui Tamura[a]

Dedicated to Professor Yoshiteru Sakata on the occasion of his 70th birthday

Abstract: To investigate dynamic solid-state complexation hitherto unexplored in nitrogen-bridged calixarene analogues, azacalix[6]arene hexamethyl ether has been prepared in three steps by applying a 5+1 fragment-coupling approach by using a Buchwald–Hartwig aryl amination reaction with the aid of our previously devised temporal N-silylation protocol. X-ray crystallographic analysis and NMR spectroscopic measurements have revealed that the azacalix[6]arene is well endowed with hydrogen-bonding ability, by which both the molecular and crystal structures are controlled. The azacalix[6]arene is conformationally flexible in solution on the NMR time scale, whereas it adopts a definite 1,2,3-alternate conformation with S_2 symmetry in the solid state as a result of intramolecular bifurcated hydrogen-bonding interactions. In the crystal, molecules of the azacalix[6]arene are mutually interacted by intermolecular hydrogen bonds to establish one-dimensional hexane-filled nanochannel crystal architecture. Although the single crystal was broken after desolvation, the resultant polycrystalline powder material was capable of selectively adsorbing CO_2 among the four main gaseous components of the atmosphere. In contrast, carbocyclic *p-tert*-butylcalix[6]arene hexamethyl ether, the crystal structure of which was also elucidated for the first time in the present study, gave rise to almost no uptake of CO_2. Additional solid–gas adsorption experiments for another three gases, such as N_2, O_2, and Ar, suggested that quadrupole/induced-dipole interactions and/or hydrogen-bonding interactions played an important role in permitting the observed selective uptake of CO_2 by this new azacalix[6]arene in the solid state.

Keywords: calixarenes · conformation analysis · structure elucidation · host–guest systems · solid–gas adsorption

Introduction

Since the pioneering and systematic studies by Gutsche, calixarenes have been playing a significant role in supramolecular chemistry together with crown ethers and cyclodextrins.[1–3] As typified by thiacalixarenes, a variety of calixarene analogues with heteroatoms as the bridging units have thus far been reported.[3–7] Interest in these analogues comes from the fact that replacement of the carbon bridges with heteroatoms can impart novel properties and functions to the molecules. In recent years, nitrogen-bridged calixarene analogues have emerged as a new calixarene family.[7] While the diversity is still limited relative to those of carbon- and sulfur-bridged calixarenes, intriguing complexation properties based on the introduction of nitrogen atoms as the bridging units have thus far been disclosed.[8–10]

For instance, Wang reported that azacalix[*m*]arene[*n*]pyridines exhibited much greater complexation ability for fullerenes C_{60} and C_{70}, relative to those of other mono-macrocyclic receptors reported to date.[8a,b,d] Wang further revealed that azacalix[4]pyridine was able to self-regulate its conformation to finely tune the cavity, in which guest species, such as a diol and a zinc ion, were incorporated.[8c,e] Yamamoto and Kanbara demonstrated that azacalix[*n*]pyridines behaved not only as a ligand for heavy-metal ions but also as an organic superbase far superior to proton sponge.[9] Very recently, we reported that azacalix[4]arene **1** exhibited selec-

[a] Dr. H. Tsue, K. Ishibashi, S. Tokita, Dr. H. Takahashi, K. Matsui, Prof. Dr. R. Tamura
Graduate School of Human and Environmental Studies
Kyoto University, Yoshida-nihonmatsu
Sakyo-ku, Kyoto 606-8501 (Japan)
Fax: (+81) 75 753 6722
E-mail: tsue@ger.mbox.media.kyoto-u.ac.jp

Supporting information for this article is available on the WWW under http://dx.doi.org/10.1002/chem.200800502.

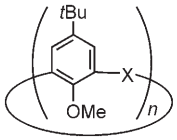

1: X = NMe, n = 4
2: X = NH, n = 6
3: X = CH_2, n = 6

tive complexation with the potassium ion due to its frozen 1,3-alternate conformation.[10] However, complexation behaviors of nitrogen-bridged calixarene analogues had been studied principally in solution, despite the fact that X-ray crystallographic analyses were performed to examine the static structures of the complexes. To the best of our knowledge, there is no precedent for the dynamic complexation studies of nitrogen-bridged calixarene analogues in the solid state, though Atwood and Barbour recently published their significant findings that carbocyclic *p-tert*-butylcalix[*n*]arenes ($n=4$ and 5) were capable of efficiently adsorbing gaseous molecules even on the nonporous crystals under ambient conditions,[11] in which the carbon-bridged calixarenes exhibited a greater adsorption ability relative to those of other new materials, such as metal-organic frameworks (MOF) and carbon nanotubes.[11i]

Solid-state complexation by nitrogen-bridged calixarene analogues is of great interest because the bridging nitrogen atoms can act not merely as additional binding sites, but also as conjugation sites with aromatic π-systems to increase the electron density of the π-cloud, thereby boosting intermolecular interactions with guest species from a molecular level, as verified by the above-mentioned complexation studies in solution. To explore whether solid-state complexation by nitrogen-bridged calixarene analogues would be feasible or not, we have synthesized azacalix[6]arene hexamethyl ether **2** in the present study, because a larger macrocycle than our previously reported azacalix[4]arene **1**[12] is essential for gaining a deeper insight into the host-guest chemistry of this molecular system. Among a variety of solid-state complexation phenomena, solid–gas adsorption behavior of **2** has been investigated in this study because it is an old, but yet forefront research area for selective gas recognition, storage, and separation, coupled with the environmental and industrial demands. As an eventual outcome, selective and rapid adsorption of CO_2 among the four main gaseous components of the atmosphere was observed on the desolvated polycrystalline powder of **2**, which was obtained from the single crystals of the hexane clathrate of **2** with a 1:1 host/guest ratio. In contrast, azacalix[4]arene **1** and carbocyclic calix[6]arene **3** exhibited almost no uptake of gaseous molecules examined herein. More interestingly, adsorption capacity of the polycrystalline powder of **2** for CO_2 was comparable to, or somewhat poorer than, those of MOFs[13] and zeolites,[14] which similarly exhibited the selective adsorption of CO_2. It has also been found from the X-ray crystallographic analysis and NMR spectroscopic measurements that azacalix[6]arene **2** with NH bridges is well endowed with hydrogen-bonding ability, by which both the molecular and crystal structures of **2** are controlled. In this paper, we report the synthesis, molecular and crystal structures, and solid–gas adsorption behavior of azacalix[6]arene **2**.

Results and Discussion

Synthesis: For the preparation of azacalix[6]arene **2**, three typical synthetic strategies are applicable that are substantially identical to those established in the carbocyclic calixarene chemistry, that is, 1) single-step synthesis, 2) nonconvergent synthesis, and 3) convergent fragment-coupling synthesis.[7] After our numerous attempts to prepare azacalix[6]arene **2**, a convergent 5+1 fragment-coupling approach, as shown in Scheme 1, was finally devised. The 5-fragment **5**

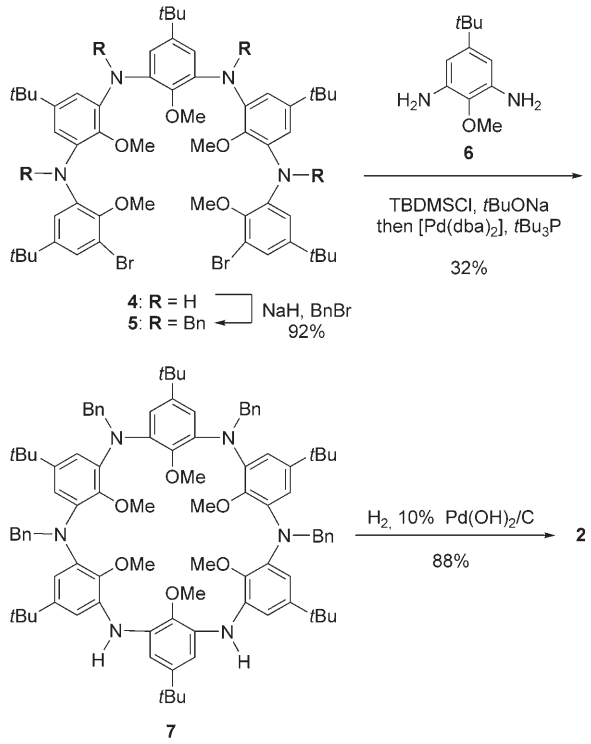

Scheme 1. Convergent 5+1 fragment-coupling synthesis of azacalix[6]arene **2**. dba = *E,E*-dibenzylideneacetone.

was prepared in 92% yield by the full N-benzylation of liner pentamer **4**.[15] To a ring-closing reaction of 5-fragment **5** with 1-fragment **6**,[16] a Buchwald–Hartwig aryl amination reaction[17] with a temporal N-silylation protocol[18] was applied, which was demonstrated to be expedient for preparing the azacalixarene with no substituent on the bridging nitrogen atoms. From this macrocyclization reaction, regioselectively tetrabenzylated azacalix[6]arene **7** was successfully obtained in 32% yield through the in-situ N,N′-bissilylation of 1-fragment **6** with *tert*-butyldimethylsilyl chloride (TBDMSCl) in the presence of *t*BuONa, followed by the one-pot Pd^0-catalyzed aryl amination reaction with the 5-fragment **5** and by the subsequent cleavage of the N–Si bond in the workup process. Final hydrogenolysis of the *N*-

benzyl groups of **7** smoothly proceeded by using 10% $Pd(OH)_2/C$ as a catalyst to give azacalix[6]arene **2** in 88% yield. FDMS, ^1H and ^{13}C NMR spectroscopy, FTIR spectroscopy, elemental analysis, and X-ray crystallographic analysis fully characterized the structure of this new azacalix[6]arene **2**.

Molecular structure in solution: In the ^1H NMR spectrum of azacalix[6]arene **2** (Figure 1a), only four sharp singlet signals were observed at $\delta = 1.27$, 3.26, 6.20, and 6.87 ppm for the

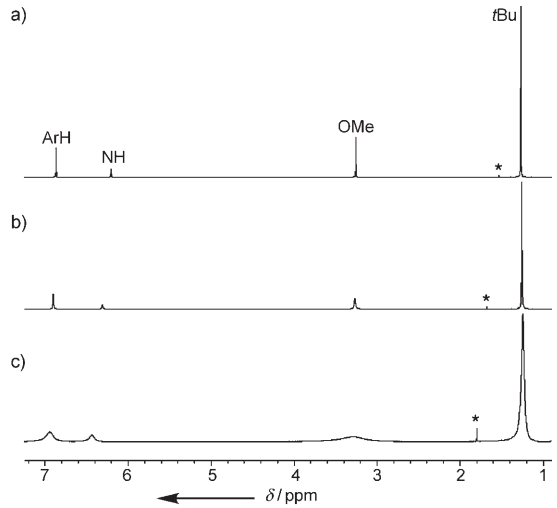

Figure 1. Temperature-dependent ^1H NMR spectra of azacalix[6]arene **2** in $CDCl_3$ at a) 25, b) −20, and c) −50 °C. Peaks marked with an asterisk are due to water.

tert-butyl, methoxy, amino, and aromatic hydrogen atoms, respectively. NH hydrogen atoms of **2** at $\delta = 6.20$ ppm experience a downfield shift relative to that of diphenylamine at $\delta = 5.6$ ppm, which indicates that the NH hydrogen atoms form hydrogen bonds with spatially adjacent methoxy groups, as revealed by the X-ray crystallographic analysis mentioned in the following section. The NMR spectroscopic signals of **2** became broad when the temperature was decreased to −20 °C (Figure 1b), but no signal splitting was observed even at −50 °C (Figure 1c), which indicates that azacalix[6]arene **2** was conformationally flexible in solution. The larger ring size of **2** is responsible for its flexibility, in contrast to azacalix[4]arene **1**, which is demonstrated to be conformationally inflexible in solution in the range of −80 to 80 °C.[10]

Crystal structure: A single crystal suitable for X-ray crystallographic analysis was obtained by slow crystallization from hexane with a few drops of CH_2Cl_2. Azacalix[6]arene **2** crystallizes with one molecule of hexane into a monoclinic form, space group $P2_1/a$ ($Z = 2$); the fundamental crystal data and experimental parameters for the structure determination are summarized in Table 1. Contrary to the flexible conformation in solution, azacalix[6]arene **2** adopts a definite 1,2,3-al-

Table 1. X-ray analytical data for azacalix[6]arene **2**, calix[6]arene **3**, and linear trimer **8**.

Compound	**2**·hexane	**3**	**8**
formula	$C_{72}H_{104}N_6O_6$	$C_{72}H_{96}O_6$	$C_{33}H_{44}Br_2N_2O_3$
M_r	1149.65	1057.55	676.53
crystal system	monoclinic	triclinic	monoclinic
space group	$P2_1/a$ (#14)	$P\bar{1}$ (#2)	$C2/c$ (#15)
a [Å]	13.7437(5)	10.6734(5)	26.027(9)
b [Å]	18.6121(8)	11.9422(7)	9.851(3)
c [Å]	15.4552(8)	14.1011(7)	25.329(9)
α [°]	–	82.442(2)	–
β [°]	111.850(1)	73.837(1)	92.05(3)
γ [°]	–	70.986(2)	–
V [Å^3]	3669.4(3)	1630.5(2)	6490(3)
Z	2	1	8
ρ [g cm^{-3}]	1.040	1.077	1.385
μ [cm^{-1}]	0.656	0.663	25.40
T [°C]	-140	-140	-100
no. of unique reflns	8346	6892	7424
no. of variables	488	380	362
$R1$[a]	0.080	0.067	0.045
$wR2$[b]	0.275	0.240	0.130
S	1.134	1.090	1.044

[a] $R1 = \Sigma||F_o| - |F_c||/\Sigma|F_o|$ for $I > 2\sigma(I)$ data. [b] $wR2 = [\Sigma[w(F_o^2 - F_c^2)^2]/\Sigma w(F_o^2)^2]^{1/2}$.

ternate conformation in the solid state, as shown in Figure 2. Its ellipsoidal shape with S_2 symmetry is in a striking contrast to the parallelogram-shaped 1,2,3-alternate conforma-

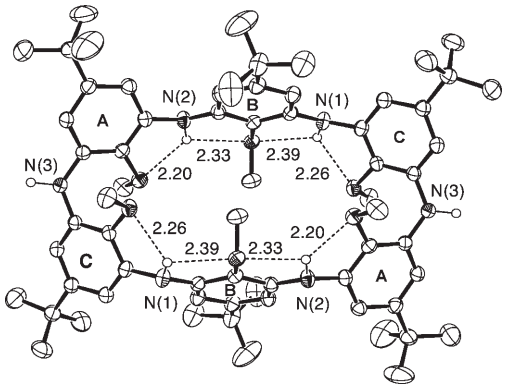

Figure 2. ORTEP drawing[20] of the hexane clathrate of azacalix[6]arene **2**. The displacement ellipsoids are drawn at the 50% probability level. Solvent molecules and all hydrogen atoms, except for the bridging NH groups are omitted for clarity. Numbers indicate O···H distances [Å] of intramolecular NH···OMe hydrogen bonds.

tion of the carbocyclic analogue **3** (Figure 3), of which the crystal structure has also been elucidated for the first time in the present study. Interestingly, the centrosymmetric 1,2,3-alternate conformation of **2** differs greatly from the highly distorted 1,3-alternate conformation of the fully N-methylated derivative of **2** (see Figure S2 in the Supporting Information).[19]

The asymmetric unit of azacalix[6]arene **2** involves half the molecule, and thus the aromatic units can be classified into three types, designated as **A**, **B**, and **C** (Figure 2). These

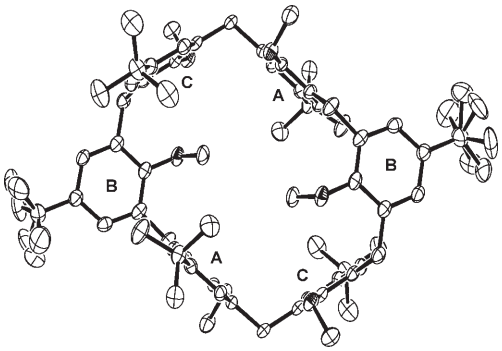

Figure 3. ORTEP drawing[20] of calix[6]arene **3** with 50% displacement ellipsoids. Hydrogen atoms are omitted for clarity.

three aromatic rings point to almost the same direction due to the presence of the two sets of intramolecular bifurcated MeO···NH···OMe hydrogen bonds formed between the aromatic rings **A** and **B**, and between the rings **B** and **C**. As shown in Figure 4, the same type of intramolecular bifurcated MeO···NH···OMe hydrogen bonds were observed for linear trimer **8**,[12] which adopted the almost coplanar arrangement of the three aromatic rings. Accordingly, azacalix[6]arene **2** can be viewed as a N(3)-bridged head-to-tail dimer of two planar trimer units **8**. NH hydrogen atoms of the N(3) atoms of **2** are directed outward from the cavity and take part in the formation of intermolecular hydrogen bonds.

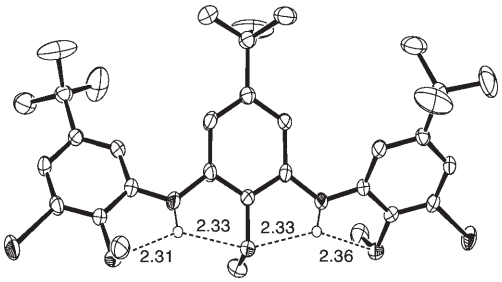

Figure 4. ORTEP drawing[20] of linear trimer **8** with 50% displacement ellipsoids. All hydrogen atoms, except for the bridging NH groups are omitted for clarity. Numbers indicate O···H distances [Å] of intramolecular NH···OMe hydrogen bonds.

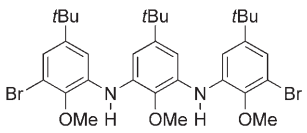

8

Another interesting point to note is the crystal packing characterized by an infinite one-dimensional (1D) solvent-filled nanochannel structure, as shown in Figure 5 and Figure S3 in the Supporting Information. In the crystal, each

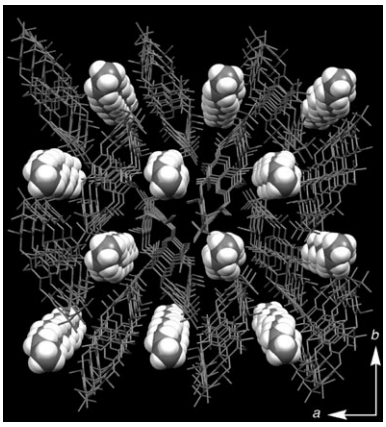

Figure 5. Crystal structure of the hexane clathrate of azacalix[6]arene **2** viewed along the *c* axis. Molecules of azacalix[6]arene **2** and hexane are represented by stick and space-filling models, respectively.

azacalix[6]arene **2** interacts with adjacent molecules by intermolecular NH/O hydrogen bonds (NH···O, 2.07 Å and 173°; N···O, 3.04 Å; see Figure 6 and Figure S4 in the Supporting Information) formed between the bridging nitrogen atoms N(3) and the methoxy groups of the aromatic ring **B** belonging to the neighboring molecule. Propagation of the intermolecular NH/O hydrogen-bonding interactions along the crystallographic [1 1 0] and [$\bar{1}$ 1 0] directions results in the formation of a two-dimensional (2D) herringbone arrangement of **2** on the *ab* plane, as shown in Figure 6 and Figure S4 in the Supporting Information. In the 2D sheet structure, each hydrogen-bonded assembly comprising of four molecules of azacalix[6]arene **2** creates an interstitial pore (ca. 200 Å^3), in which one molecule of hexane with an all-anti conformation is embedded by weak intermolecular CH/O interactions (CH···O, 2.98 Å and 149°; C···O, 3.85 Å; Figure 7) between the methylene group of hexane and the methoxy group of the ring **B**. As a result, the hexane-filled 2D sheet structure is stacked along the *c* axis to form the 1D nanochannel crystal architecture of the hexane clathrate of **2** with a 1:1 host-guest ratio, as shown in Figure 5 and Figure S3 in the Supporting Information.

Preparation of desolvated crystal: Prior to the preparation of desolvated crystal, thermogravimetric analysis was carried out to examine the thermal stability of the hexane clathrate of **2**. As shown in Figure 8, upon heating the single crystals of the hexane clathrate, the weight of the crystals was gradually decreased to reach a constant value above 140 °C. The observed overall weight change of 7.4% was equivalent to the loss of one molecule of hexane, which indicated the complete escape of the molecules of hexane from the single crystals of **2**. Desolvation was also feasible by heating the single crystals of the hexane clathrate of **2** at 60 °C for 13 h under reduced pressure. After desolvation, however, the hexane clathrate lost the single crystallinity and turned to colorless polycrystalline powder **2P**. The letter **P** is used below to represent the solvent-free polycrystalline powder

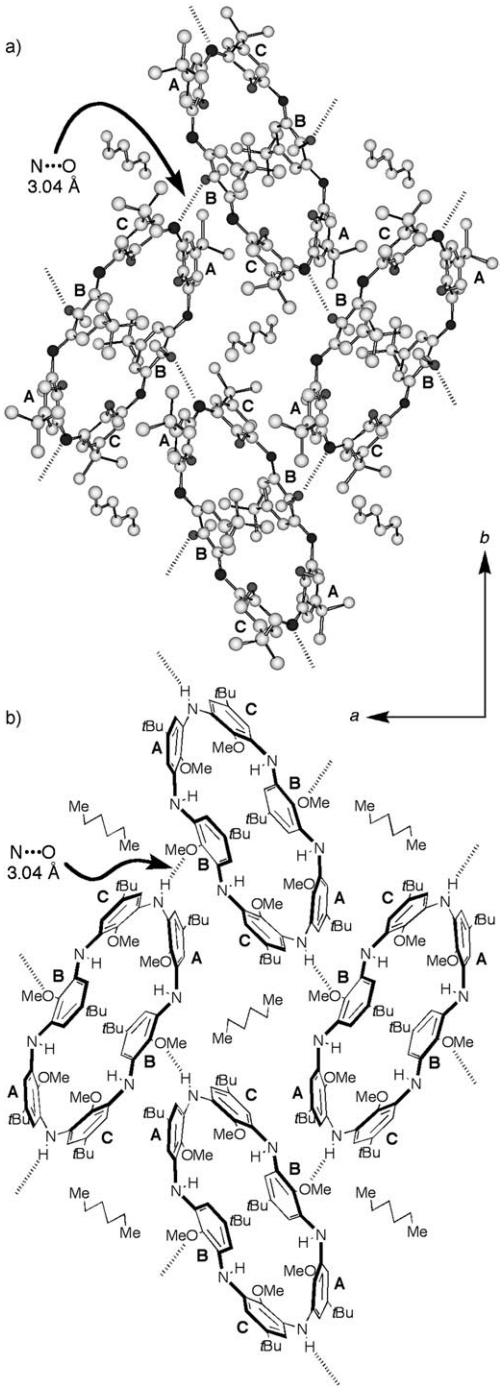

Figure 6. a) Ball-and-stick and b) schematic representations of the two-dimensional sheet structure of the hexane clathrate of azacalix[6]arene **2** on the *ab* plane. In panel (a), the carbon atoms are depicted by light-gray circles, and gray circles stand for the nitrogen and oxygen atoms. In panels (a) and (b), intermolecular NH···OMe hydrogen bonds are illustrated by dotted lines.

material obtained from the single crystals of the hexane clathrates of **2**.

The powder XRD pattern of **2P** (Figure 9a and Figure S1 in the Supporting Information) displays a similarity to the XRD patterns simulated from the X-ray crystallographic

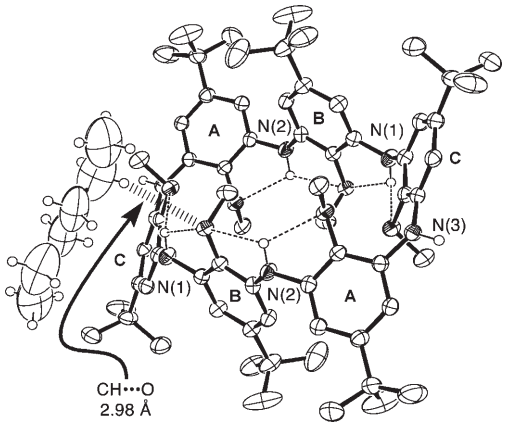

Figure 7. ORTEP drawing[20] of the hexane clathrate of azacalix[6]arene **2** with 50% displacement ellipsoids. All hydrogen atoms, except for hexane and the bridging NH groups are omitted for clarity. Number indicates the distance of the CH/O interaction between hexane and the methoxy group of the ring **B**.

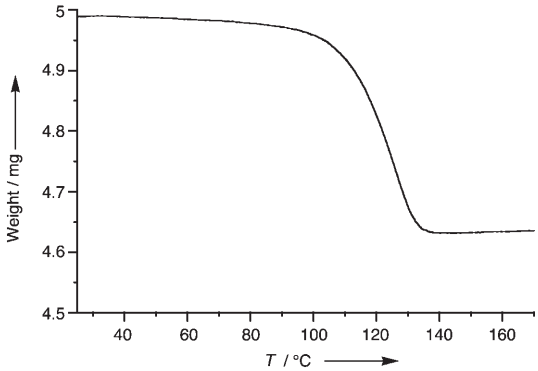

Figure 8. Thermogravimetric analysis of the hexane clathrate of azacalix[6]arene **2** recorded at 5 °C min^{-1}.

data of the hexane clathrate of **2** (Figure 9b) and also from the imaginary crystal structure simply created by deleting the atomic coordinates of hexane from the crystallographic data of the hexane clathrate (Figure 9c). Although the crystal structure of the polycrystalline powder **2P** could not be solved from the XRD pattern at this moment, FTIR measurement of **2P** revealed no appreciable change in the NH-stretching, NH-bending, and CN-stretching bands, even after the loss of single crystallinity (Figure 10), which suggested that the hydrogen bonding network observed in the single crystal (Figure 6 and Figure S4 in the Supporting Information) remained almost unchanged in polycrystalline powder **2P**. From these experimental facts, it is conceivable that, upon heating the single crystals of the hexane clathrate of **2**, molecules of hexane escape through the 1D nanochannel almost keeping the inter- and intramolecular hydrogen-bonding interactions, though azacalix[6]arene **2** should alter its 1,2,3-alternate conformation to some extent and/or undergo slight translations in the solid state.

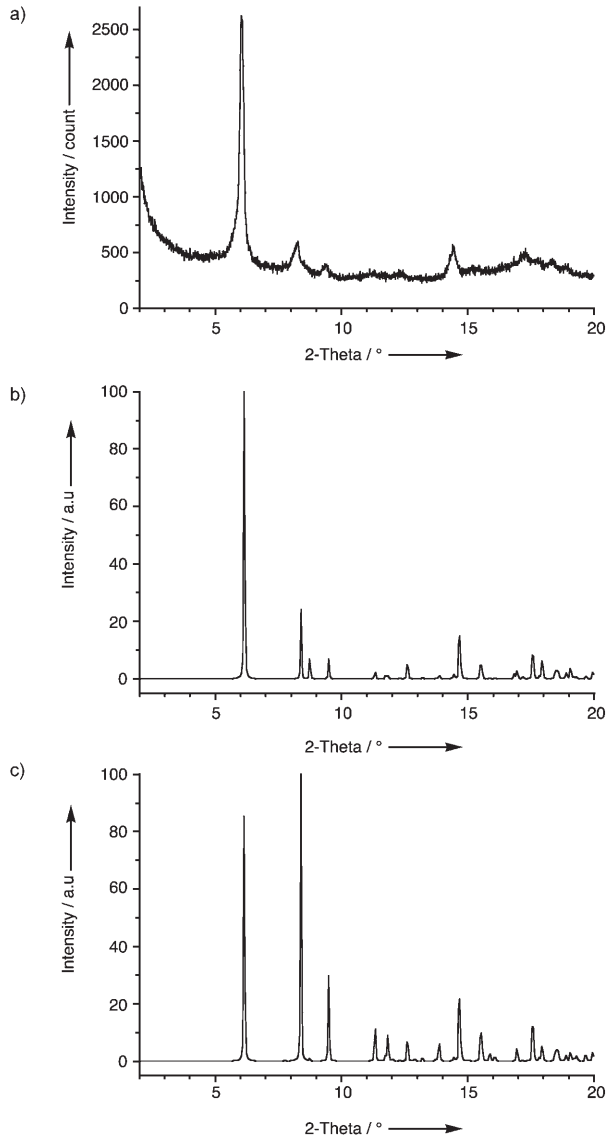

Figure 9. a) Powder XRD pattern of polycrystalline powder **2P**. b) XRD pattern simulated from the X-ray crystallographic data of the hexane clathrates of **2**. c) XRD pattern simulated from the imaginary crystal structure simply created by deleting the atomic coordinates of hexane from the crystallographic data of the hexane clathrate of **2**.

Solid–gas adsorption behavior: To gain an insight into the ability of polycrystalline powder **2P** to function as a nanoporous material, adsorption experiments for gaseous molecules were carried out. According to the described procedure,[11c] adsorption isotherms for the four main atmospheric components, such as N_2, O_2, Ar, and CO_2 were recorded at room temperature and 195 K on desolvated colorless polycrystalline powder **2P**, which was prepared by heating the single crystals of the hexane clathrate of **2** at 60 °C for 13 h under reduced pressure. The initial pressure was set to ca. 100 kPa in all adsorption experiments. At room temperature (Figure 11a and Figure S5a in the Supporting Information), no uptake was observed for all of the examined gases except for CO_2, which was slightly adsorbed on polycrystalline

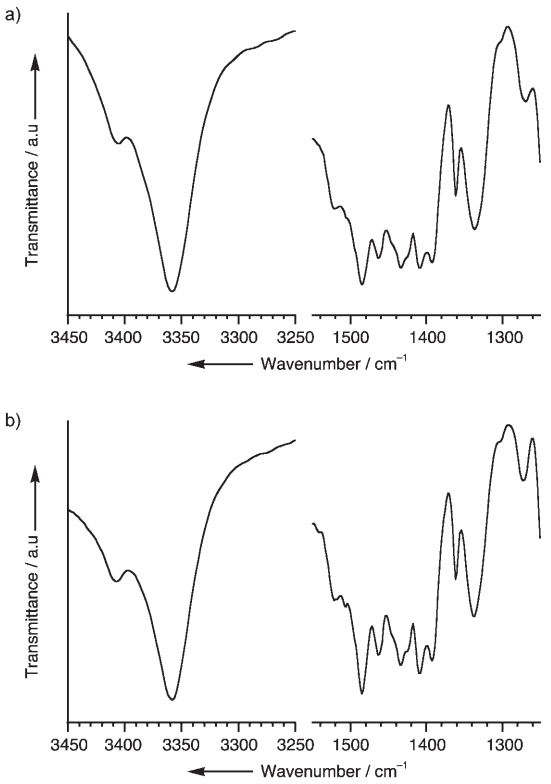

Figure 10. FTIR spectra of a) polycrystalline powder **2P** and b) the single crystals of the hexane clathrate of azacalix[6]arene **2**.

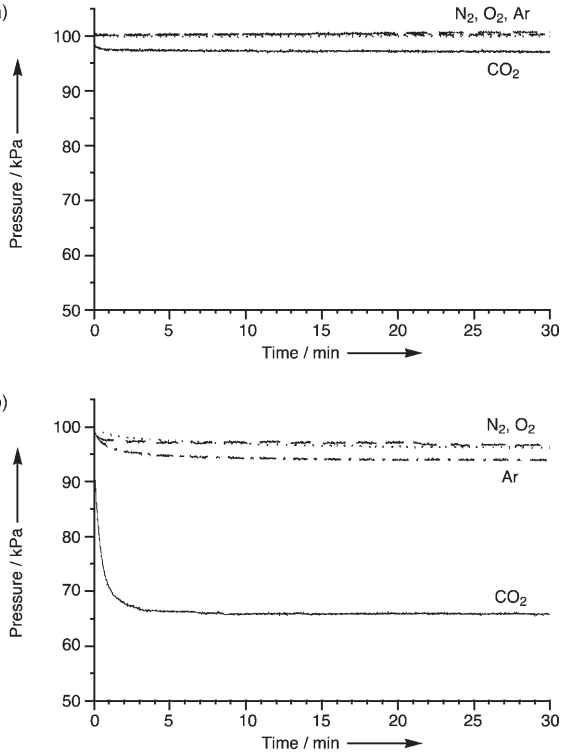

Figure 11. Gas adsorption isotherms recorded at a) room temperature and b) 195 K for CO_2, N_2, O_2, and Ar by using polycrystalline powder **2P** as an adsorbent. Isotherms for N_2, O_2, Ar, and CO_2 are shown by ••••, -----, –•–•, and ——, respectively.

powder **2P**. In contrast, CO_2 was rapidly and selectively adsorbed on **2P** at 195 K (Figure 11b and Figure S5b in the Supporting Information), and the initial pressure of ca. 100 kPa was decreased within 10 min to reach equilibrium at 65 kPa, which corresponded to the uptake of ca. 1.8 mol of CO_2 per mol of **2** (i.e. 37 $cm^3 g^{-1}$ at standard temperature and pressure). It is interesting to note that the observed adsorption capacity of **2P** for CO_2 is comparable to, or somewhat poorer than, those of MOFs[13] and zeolites[14] similarly capable of selectively adsorbing CO_2. On the whole, the observed gas adsorption behavior of **2P** at 195 K was correlated fairly well with the molecular sieve effect[21] based on the difference in the kinetic diameters of the examined gases, such as N_2 (3.64 Å), O_2 (3.46 Å), Ar (3.40 Å), and CO_2 (3.3 Å).

As a control, adsorption experiments were performed for azacalix[4]arene **1** and carbocyclic calix[6]arene **3**, the former of which was densely packed in the crystal solely by intermolecular CH/π interactions to form a nonporous crystal structure with no solvent molecule in the lattice.[12] As shown in Figure 12 and Figure S6 in the Supporting Information, carbocyclic calix[6]arene **3** also retains a nonporous and nonsolvated crystal structure, which is characterized by a 1D chain structure established by intermolecular CH/O interactions (CH···O, 2.61 Å and 126°; C···O, 3.28 Å) between the methoxy group of the aromatic ring **C** and that of ring **B** belonging to the nearest molecules. As anticipated from their densely-packed nonporous crystal structures, both azacalix[4]arene **1** and calix[6]arene **3** gave rise to almost no uptake of CO_2 even at 195 K, as shown in Figure 13 and Figure S7 in the Supporting Information. Although gas sorption was reported to happen even by nonporous materials,[11,22] the absence of interstitial void space enough to accommodate gaseous molecules in the crystal lattices of **1** and **3** would be responsible for the observed non-uptake of CO_2 by these crystalline powder materials. In other words, an infinite 1D nanochannel crystal structure observed in the single crystal of the hexane clathrate of **2** would be retained, though presumably imperfectly, in the desolvated polycrystalline powder **2P**, as suggested by the XRD and FTIR measurements (Figures 9 and 10).

Selective and rapid uptake of CO_2 by polycrystalline powder **2P** at 195 K can be explained by considering 1) hydrogen-bonding interactions and/or 2) quadrupole/induced-dipole interactions between **2** and CO_2, in addition to the molecular sieve effects mentioned above. The desolvation-induced disintegration of the single crystals of the hexane clathrate of **2** into polycrystalline powder **2P** would break a portion of the NH hydrogen bonds and change them into dangling bonds, thereby leading to the formation of hydrogen bonds with CO_2 molecules diffused into the 1D nanochannel of **2P**. This is parallel to the experimental fact that azacalix[4]arene **1** and calix[6]arene **3** lead to almost no uptake of CO_2 (Figure 13 and Figure S7 in the Supporting Information) because of the lack of hydrogen bonding sites, together with their densely-packed crystal structures. As an additional factor, quadrupole/induced-dipole interactions

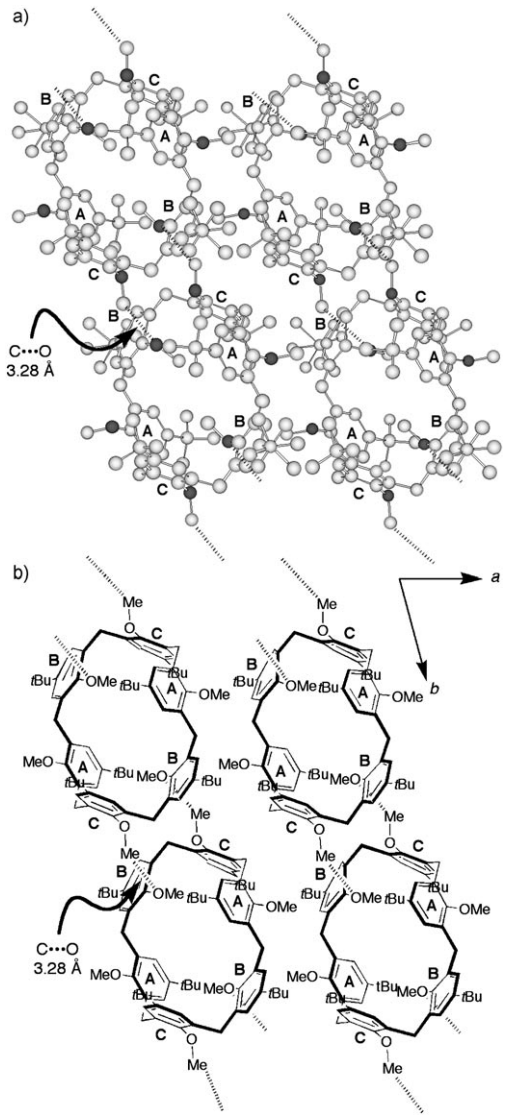

Figure 12. a) Ball-and-stick and b) schematic representations of the one-dimensional chain structure of calix[6]arene **3** along the *b* axis. In panel (a), the carbon atoms are depicted by light-gray circles, and gray circles stand for the oxygen atoms. In panels (a) and (b), intermolecular CH/O interactions are illustrated by dottted lines.

between CO_2 and the surrounding aromatic "walls" built along the 1D nanochannel of **2P** would also be involved in the selective adsorption of CO_2, judging from the greater quadrupole moment (absolute value)[23] of CO_2 (13.4×10^{40} C m^2) than the other examined gases, such as N_2 (4.7×10^{40}), O_2 (1.3×10^{40}), and Ar (0). This intermolecular interaction must also contribute to the gas adsorption behavior of carbocyclic calix[6]arene **3**, which exhibits the slight uptake of CO_2 at 195 K (Figure 13b and Figure S7b in the Supporting Information). As a result, it is conceivable that hydrogen-bonding interactions and/or quadrupole/induced-dipole interactions are responsible for the observed selective and rapid uptake of CO_2 by **2P**. Nevertheless, these intermolecular interactions are insufficient to efficiently entrap and hold CO_2 molecules in the nanochannel space of **2P** at ambient

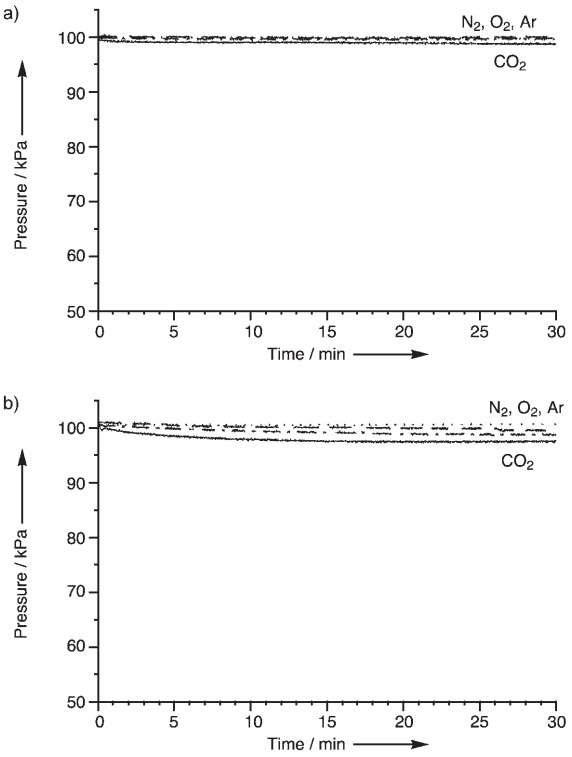

Figure 13. Gas adsorption isotherms recorded at 195 K for CO_2, N_2, O_2, and Ar by using crystalline powder materials of a) azacalix[4]arene **1** and b) carbocyclic calix[6]arene **3** as adsorbents. Isotherms for N_2, O_2, Ar, and CO_2 are shown by ••••, -----, –•–•, and ——, respectively.

temperature, as can be seen from the experimental results shown in Figure 11 and Figure S5 in the Supporting Information.

Conclusions

The present study has demonstrated that azacalix[6]arene **2** can be prepared in a simple and efficient manner by applying a Pd^0-catalyzed aryl amination reaction by using our previously devised temporal N-silylation protocol. X-ray crystallographic analysis and NMR spectroscopic measurements have clearly revealed that azacalix[6]arene **2** with NH bridges is well endowed with hydrogen-bonding ability, which controls both the molecular and crystal structures of **2**. In fact, NH hydrogen atoms of **2** experience a downfield shift in the ^{1}H NMR spectrum because of the presence of the intramolecular hydrogen-bonding interaction, by which azacalix[6]arene **2** adopts a 1,2,3-alternate conformation with S_2 symmetry in the solid state. In the crystal, molecules of **2** are mutually interacted by intermolecular hydrogen bonds to establish the infinite 1D nanochannel crystal architecture of the hexane clathrate with a 1:1 host/guest ratio. After desolvation, the resultant polycrystalline powder material **2P** was capable of selectively and rapidly adsorbing CO_2 among the four main components of the atmosphere, as a result of hydrogen-bonding interactions and/or quadrupole/induced-dipole interactions between **2** and CO_2 in the 1D nanochannel of **2P**. As an eventual outcome, the present study has clearly demonstrated that the selective solid-state complexation of gaseous CO_2 by a nitrogen-bridged calixarene analogue is feasible.

Because azacalix[6]arene **2** possesses electron-rich π-systems and the striking hydrogen-bonding ability to act as both donor and acceptor, there appears a fair prospect that azacalix[6]arene **2** may exhibit a greater gas adsorption capacity with the aid of crystal engineering. This legitimate anticipation strongly compels us to further study the solid–gas adsorption behavior of **2** and its homologues with smaller and larger ring sizes. Investigations along this line are currently under progress to gain a deeper insight into the dynamic solid-state complexation of this molecular system.

Experimental Section

General: Melting points were determined on a Yanaco MP-J3 apparatus and are uncorrected. NMR spectra were recorded on a JEOL JNM-A500 instrument by using tetramethylsilane (^{1}H NMR spectra) and solvent resonance (^{13}C NMR spectra) as internal standards. IR spectra were obtained on a Shimadzu IRPrestige-21 spectrometer. Mass spectra were recorded at the GCMS and NMR Laboratory, Faculty of Agriculture, Hokkaido University (Japan). Elemental analyses were conducted at the Microanalytical Center, Kyoto University (Japan). Thermogravimetric analysis was performed with a Shimadzu TGA-50 instrument at the scanning rate of 5 °C min^{-1}. Powder XRD patterns were recorded by a Rigaku RINT 2200 diffractometer by using $Cu_{K\alpha}$ radiation ($\lambda = 1.54056$ Å, 40 kV, 40 mA) with a graphite monochrometor at a step width of 0.01° 2θ and a counting time of 2 s step^{-1}. Flash column chromatography was performed with Kanto Silica Gel 60N (40–50 μm). Toluene, CH_2Cl_2, and DMF were refluxed over and then distilled from CaH_2 under Ar before use. Palladium bis(benzylideneacetone) ([Pd(dba)$_2$]),[24] calix[6]arene **3**,[25] and compounds **4**[15], **6**[16], and **8**[12] were prepared according to the described procedure. Other chemicals were purchased from commercial suppliers and used as received.

***N*,*N*′-Bis[3-(*N*″-benzyl-3-bromo-5-*tert*-butyl-2-methoxyanilino)-5-*tert*-butyl-2-methoxyphenyl]-*N*,*N*′-dibenzyl-5-*tert*-butyl-2-methoxy-1,3-phenylenediamine (5)**: 60% NaH (481 mg, 12.0 mmol) was added to a solution of **4**[15] (2.06 g, 2.00 mmol) in anhydrous DMF (40 mL) at 0 °C under Ar. After the reaction mixture had been stirred for 5 min, BnBr (1.1 mL, 9.0 mmol) was added. Stirring was continued at room temperature overnight, and then Et_2O was added to the reaction mixture. The organic layer was washed with brine, dried over Na_2SO_4, filtered, and evaporated. Flash column chromatography on silica gel (hexane/CH_2Cl_2 3:1) and subsequent precipitation from Et_2O/MeOH gave **5** (2.56 g, 92%) as a pale-pink solid. M.p. 103–105 °C; ^{1}H NMR (500 MHz, $CDCl_3$): $\delta = 7.28$–7.08 (m, 20H; ArH), 7.06 (d, ^4J(H,H) = 2.3 Hz, 2H; ArH), 6.86 (d, ^4J(H,H) = 2.3 Hz, 2H; ArH), 6.70 (d, ^4J(H,H) = 2.3 Hz, 2H; ArH), 6.62 (s, 2H; ArH), 6.59 (d, ^4J(H,H) = 2.3 Hz, 2H; ArH), 4.81 (s, 4H; NCH_2Ph), 4.80 (s, 4H; NCH_2Ph), 3.461 (s, 3H; OMe), 3.457 (s, 6H; OMe), 3.41 (s, 6H; OMe), 1.11 (s, 18H; *t*Bu), 1.03 (s, 18H; *t*Bu), 1.02 ppm (s, 9H; *t*Bu); ^{13}C NMR (125 MHz, $CDCl_3$): $\delta = 148.1$, 147.4, 145.7, 145.23, 145.21, 145.0, 143.2, 142.7, 142.6, 139.4, 128.04, 127.99, 127.97, 127.9, 126.5, 126.2, 123.2, 119.9, 117.5, 117.1, 117.0, 116.3, 59.9, 59.13, 59.10, 56.9, 56.7, 34.4, 34.28, 34.27, 31.14, 31.13, 31.08 ppm; elemental analysis calcd (%) for $C_{83}H_{98}Br_2N_4O_5$: C 71.64, H 7.10, N 4.03; found: C 71.72, H 7.09, N 3.99.

***N*,*N*′,*N*″,*N*‴-Tetrabenzyl-5,11,17,23,29,35-hexa-*tert*-butyl-37,38,39,40,41,42-hexamethoxy-2,8,14,20,26,32-hexaazacalix[6]arene (7)**: A solution of **5** (696 mg, 500 μmol), **6**[16] (97.2 mg, 500 μmol), *t*BuONa (240 mg, 2.50 mmol), and TBDMSCl (151 mg, 1.00 mmol) in anhydrous toluene (100 mL) was stirred at 80 °C under Ar. After the reaction mix-

ture had been stirred for 30 min, [Pd(dba)$_2$] (57.4 mg, 100 μmol) and 10 wt% tBu$_3$P in hexane (240 μL, 80 μmol) were added. The solution was refluxed for 22 h and then cooled to room temperature. The reaction mixture was passed through Celite and evaporated. Flash column chromatography on silica gel (hexane/CH_2Cl_2 1:1) and subsequent washing with Et_2O/MeOH gave **7** (227 mg, 32%) as a colorless solid. M.p. 256–257 °C (dec.); ^{1}H NMR (500 MHz, $CDCl_3$): $\delta = 7.36$ (d, ^3J(H,H) = 7.3 Hz, 4H; ArH), 7.29 (d, ^3J(H,H) = 7.3 Hz, 4H; ArH), 7.24–7.21 (m, 6H; ArH), 7.16–7.15 (m, 6H; ArH), 7.11 (brs, 2H; ArH), 7.07 (brs, 2H; ArH), 6.97 (brs, 2H; ArH), 6.79 (brs, 2H; ArH), 6.54 (brs, 2H; ArH), 6.35 (brs, 2H; NH), 5.19–4.77 (m, 8H; NCH_2Ph), 3.70 (brs, 3H; OMe), 3.28 (brs, 6H; OMe), 2.60 (brs, 6H; OMe), 2.24 (brs, 3H; OMe), 1.32 (brs, 9H; tBu), 1.30 (brs, 18H; tBu), 1.15 (s, 18H; tBu), 1.12 ppm (s, 9H; tBu); ^{13}C NMR (125 MHz, $CDCl_3$): $\delta = 149.6$, 146.5, 145.7, 145.5, 145.0, 142.0, 140.0, 139.6, 138.9, 138.2, 137.9, 136.5, 130.0, 128.4, 127.8, 127.6, 126.8, 126.5, 121.2, 117.2, 113.7, 112.5, 109.5, 100.9, 60.3, 60.0, 59.6, 59.5, 59.2, 58.9, 34.58, 34.56, 34.52, 34.4, 31.5, 31.40, 31.36, 31.1 ppm; IR (KBr): 3361 cm^{-1} (ν_{NH}); elemental analysis calcd (%) for $C_{94}H_{114}N_6O_6$: C 79.29, H 8.07, N 5.90; found: C 79.54, H 8.23, N 5.80.

5,11,17,23,29,35-Hexa-*tert*-butyl-37,38,39,40,41,42-hexamethoxy-2,8,14,20, 6]arene (2): A solution of **7** (427 mg, 300 μmol) and 10% Pd(OH)$_2$/C (204 mg) in cyclohexane (50 mL) was stirred at room temperature under H_2 (3.9 atm). After the reaction mixture had been stirred for 31 h, additional 10% Pd(OH)$_2$/C (200 mg) was added, and then stirring was continued for another 14 h under H_2 (4.0 atm). The reaction mixture was passed through Celite and evaporated. Flash column chromatography on silica gel (hexane/CH_2Cl_2 1:1 then 1:2) and recrystallization from CH_2Cl_2/hexane gave **2** (280 mg, 88%) as a colorless solid. M.p. 295–296 °C (dec.); ^{1}H NMR (500 MHz, $CDCl_3$): $\delta = 6.87$ (s, 12H; ArH), 6.20 (s, 6H; NH), 3.26 (s, 18H; OMe), 1.27 ppm (s, 54H; tBu); ^{13}C NMR (125 MHz, $CDCl_3$): $\delta = 146.5$, 139.5, 137.6, 110.4, 59.6, 34.5, 31.4 ppm; IR (KBr) 3358, 3406 cm^{-1} (ν_{NH}); MS (FD): m/z (%): 1063 (100) [M^+], 531 (9) [M^{2+}], 354 (2) [M^{3+}]; elemental analysis calcd (%) for $C_{66}H_{90}N_6O_6$: C 74.54, H 8.53, N 7.90; found: C 74.33, H 8.58, N 7.83.

Gas adsorption experiments: By reference to the literature of Atwood and Barbour,[11c] essentially the same devise was constructed to record solid–gas absorption isotherms of **1** (10.4 mg), **2P** (19.7 mg), and **3** (19.4 mg) at room temperature and 195 K. The powder material was placed in a sample chamber, and then both sample and reference chambers (each volume = 2.0 cm^3) were evacuated at 1 kPa for 1 h. After the chambers were pressurized to ca. 100 kPa by the desired gas, their internal pressures were monitored by using two pressure transducers (Swagelok PTI-S-MC.15–15AQ-A) attached to each chamber. Adsorption equilibrium was reached within 20 min, and the gas adsorption capacity was estimated from the changes in pressure.

X-ray crystallographic analyses: The X-ray data were collected on a Rigaku RAXIS RAPID diffractometer with graphite-monochromated $Mo_{K\alpha}$ radiation ($\lambda = 0.71075$ Å) to $2\theta_{max}$ of 54.9° for **2**·hexane and of 55.0° for **3** and **8**. All the crystallographic calculations were performed by using a crystallographic software package, CrystalStructure, Version 3.8.2.[26] The crystal structure was solved by direct methods and refined by full-matrix least-squares. All non-hydrogen atoms were refined anisotropically, and hydrogen atoms were refined by using the riding model. The fundamental crystal data and experimental parameters for the structure determination are given in Table 1. CCDC-681115, 681116, and 681117 contain the supplementary crystallographic data for this paper. These data can be obtained free of charge from The Cambridge Crystallographic Data Centre via www.ccdc.cam.ac.uk/data_request/cif.

Acknowledgements

This work was supported by a Grant-in-Aid for Scientific Research (no. 19550037 to H.T.) from the Ministry of Education, Culture, Sports, Science and Technology, Japan. We are grateful to the GCMS and NMR Laboratory, Faculty of Agriculture, Hokkaido University for FD MS measurements.

[1] a) C. D. Gutsche, *Calixarenes* (Ed.: J. F. Stoddart), The Royal Society of Chemistry, Cambridge, **1989**; b) C. D. Gutsche, *Calixarenes Revisited* (Ed.: J. F. Stoddart), The Royal Society of Chemistry, Cambridge, **1998**.

[2] *Calixarenes: A Versatile Class of Macrocyclic Compounds* (Eds.: J. Vicens, V. Böhmer), Kluwer, Dordrecht, **1991**.

[3] *Calixarenes 2001* (Eds.: Z. Asfari, V. Böhmer, J. Harrowfield, J. Vicens, M. Saadioui), Kluwer, Dordrecht, **2001**.

[4] B. König, M. H. Fonseca, *Eur. J. Inorg. Chem.* **2000**, 2303.

[5] P. Lhoták, *Eur. J. Org. Chem.* **2004**, 1675.

[6] N. Morohashi, F. Narumi, N. Iki, T. Hattori, S. Miyano, *Chem. Rev.* **2006**, *106*, 5291.

[7] H. Tsue, K. Ishibashi, R. Tamura in *Heterocyclic Supramolecules* (Ed.: K. Matsumoto), *Topics in Heterocyclic Chemistry*, Springer, Heidelberg, in press..

[8] a) M.-X. Wang, Z.-H. Zhang, Q.-Y. Zheng, *Angew. Chem.* **2004**, *116*, 856; *Angew. Chem. Int. Ed.* **2004**, *43*, 838; b) H.-Y. Gong, X.-H. Zhang, D.-X. Wang, H.-W. Ma, Q.-Y. Zheng, M.-X. Wang, *Chem. Eur. J.* **2006**, *12*, 9262; c) H.-Y. Gong, Q.-Y. Zheng, X.-H. Zhang, D.-X. Wang, M.-X. Wang, *Org. Lett.* **2006**, *8*, 4895; d) S.-Q. Liu, D.-X. Wang, Q.-Y. Zheng, M.-X. Wang, *Chem. Commun.* **2007**, 3856; e) H.-Y. Gong, D.-X. Wang, J.-F. Xiang, Q.-Y. Zheng, M.-X. Wang, *Chem. Eur. J.* **2007**, *13*, 7791.

[9] a) Y. Miyazaki, T. Kanbara, T. Yamamoto, *Tetrahedron Lett.* **2002**, *43*, 7945; b) Y. Suzuki, T. Yanagi, T. Kanbara, T. Yamamoto, *Synlett* **2005**, 263; c) T. Kanbara, Y. Suzuki, T. Yamamoto, *Eur. J. Org. Chem.* **2006**, 3314.

[10] H. Tsue, K. Ishibashi, S. Tokita, K. Matsui, H. Takahashi, R. Tamura, *Chem. Lett.* **2007**, *36*, 1374.

[11] a) J. L. Atwood, L. J. Barbour, A. Jerga, *Science* **2002**, *296*, 2367; b) J. L. Atwood, L. J. Barbour, A. Jerga, *Angew. Chem.* **2004**, *116*, 3008; *Angew. Chem. Int. Ed.* **2004**, *43*, 2948; c) J. L. Atwood, L. J. Barbour, P. K. Thallapally, T. B. Wirsig, *Chem. Commun.* **2005**, 51; d) P. K. Thallapally, T. B. Wirsig, L. J. Barbour, J. L. Atwood, *Chem. Commun.* **2005**, 4420; e) P. K. Thallapally, G. O. Lloyd, T. B. Wirsig, M. W. Bredenkamp, J. L. Atwood, L. J. Barbour, *Chem. Commun.* **2005**, 5272; f) L. Dobrzanska, G. O. Lloyd, H. G. Raubenheimer, L. J. Barbour, *J. Am. Chem. Soc.* **2006**, *128*, 698; g) P. K. Thallapally, L. Dorbrzanska, T. R. Gingrich, T. B. Wirsig, L. J. Barbour, J. L. Atwood, *Angew. Chem.* **2006**, *118*, 6656; *Angew. Chem. Int. Ed.* **2006**, *45*, 6506; h) P. K. Thallapally, S. J. Dalgarno, J. L. Atwood, *J. Am. Chem. Soc.* **2006**, *128*, 15060; i) P. K. Thallapally, K. A. Kirby, J. L. Atwood, *New J. Chem.* **2007**, *31*, 628; j) S. J. Dalgarno, P. K. Thallapally, L. J. Barbour, J. L. Atwood, *Chem. Soc. Rev.* **2007**, *36*, 236; k) P. K. Thallapally, B. P. McGrail, J. L. Atwood, *Chem. Commun.* **2007**, 1521; l) P. K. Thallapally, B. P. McGrail, J. L. Atwood, C. Gaeta, C. Tedesco, P. Neri, *Chem. Mater.* **2007**, *19*, 3355; m) S. J. Dalgarno, J. Tian, J. E. Warren, T. E. Clark, M. Makha, C. L. Raston, J. L. Atwood, *Chem. Commun.* **2007**, 4848; n) P. K. Thallapally, B. P. McGrail, S. J. Dalfarno, H. T. Schaef, J. Tian, J. L. Atwood, *Nat. Mater.* **2008**, *7*, 146.

[12] H. Tsue, K. Ishibashi, H. Takahashi, R. Tamura, *Org. Lett.* **2005**, *7*, 2165.

[13] a) L. Pan, K. M. Adams, H. E. Herrandez, X. Wang, C. Zheng, Y. Hattori, K. Kaneko, *J. Am. Chem. Soc.* **2003**, *125*, 3062; b) D. N. Dybtsev, H. Chun, S. H. Yoon, D. Kim, K. Kim, *J. Am. Chem. Soc.* **2004**, *126*, 32; c) S. M. Humphrey, J.-S. Chang, S. H. Jhung, J. W. Yoon, P. T. Wood, *Angew. Chem.* **2006**, *118*, 276; *Angew. Chem. Int. Ed.* **2006**, *46*, 272; d) P. L. Llewellyn, S. Bourrelly, C. Serre, Y. Filinchuk, G. Férey, *Angew. Chem.* **2006**, *118*, 7915; *Angew. Chem. Int. Ed.* **2006**, *455*, 7751; e) S. Ma, D. Sun, X.-S. Wang, H.-C. Zhou, *Angew. Chem.* **2007**, *119*, 2510; *Angew. Chem. Int. Ed.* **2007**, *46*, 2458; f) J. W. Sung, S. H. Jhung, Y. K. Hwang, S. M. Humphrey, P. T. Wood, J.-S. Chang, *Adv. Mater.* **2007**, *19*, 1830; g) B. Chen, S. Ma, F. Zapata, F. R. Fronczek, E. B. Lobkovsky, H.-C. Zhou, *Inorg. Chem.* **2007**, *46*, 1233; h) Y. Zou, S. Hong, M. Park, H. Chun, S. Lah, *Chem. Commun.* **2007**, 5182.

[14] a) V. R. Choudhary, S. Mayadevi, A. P. Singh, *J. Chem. Soc. Faraday Trans.* **1995**, 2935; b) J. A. Dunne, M. Rao, S. Sircar, R. J. Gorte, A. L. Myers, *Langmuir* **1996**, *12*, 5896; c) M. Katoh, T. Yoshikawa, T. Tomonari, K. Katayama, T. Tomida, *J. Colloid Interface Sci.* **2000**, *226*, 145; d) R. V. Siriwardane, M.-S. Shen, E. P. Fischer, J. A. Poston, *Energy Fuels* **2001**, *15*, 279; e) S. Pakseresht, M. Kazemeini, M. M. Akbarnejad, *Sep. Purif. Technol.* **2002**, *28*, 53; f) E. D. Akten, R. Siriwardane, D. S. Sholl, *Energy Fuels* **2003**, *17*, 977.
[15] K. Ishibashi, H. Tsue, N. Sakai, S. Tokita, K. Matsui, J. Yamauchi, R. Tamura, *Chem. Commun.*, in press.
[16] S. Breitfelder, P. F. Cirillo, J. R. Regan, Boehringer Ingelheim Pharmaceuticals Inc. , PCT Int. Appl. WO 200283642, **2002** [*Chem. Abstr.* **2002**, *137*, 325421].
[17] For reviews on palladium(0)-catalyzed aryl amination reactions: a) J. P. Wolfe, S. Wagaw, J. F. Marcoux, S. L. Buchwald, *Acc. Chem. Res.* **1998**, *31*, 805; b) J. F. Hartwig, *Acc. Chem. Res.* **1998**, *31*, 852; c) J. F. Hartwig, *Angew. Chem.* **1998**, *110*, 2154; *Angew. Chem. Int. Ed.* **1998**, *37*, 2046; d) A. R. Muci, S. L. Buchwald, *Top. Curr. Chem.* **2002**, *219*, 133.
[18] K. Ishibashi, H. Tsue, S. Tokita, K. Matsui, H. Takahashi, R. Tamura, *Org. Lett.* **2006**, *8*, 5991.
[19] K. Ishibashi, H. Tsue, H. Takahashi, S. Tokita, K. Matsui, R. Tamura, *Heterocycles*, in press.
[20] L. J. Farrugia, *J. Appl. Crystallogr.* **1997**, *30*, 565.
[21] D. W. Breck, *Zeolite Molecular Sieves*, Wiley, New York, **1974**, pp. 633–645.
[22] J. A. Riddle, J. C. Bollinger, D. Lee, *Angew. Chem.* **2005**, *117*, 6847; *Angew. Chem. Int. Ed.* **2005**, *44*, 6689.
[23] W. Steele, *Chem. Rev.* **1993**, *93*, 2355.
[24] T. Ukai, H. Kawazura, Y. Ishii, J. J. Bonnet, J. A. Ibers, *J. Organomet. Chem.* **1974**, *65*, 253.
[25] C. D. Gutsche, L.-G. Lin, *Tetrahedron* **1986**, *42*, 1633.
[26] CrystalStructure, Version 3.8.2, Rigaku and Rigaku Americas, The Woodlands, TX (USA), **2000–2007**.

Received: March 18, 2008
Published online: May 28, 2008

